Atmospheric Lifetimes and Global Warming Potentials of Hydrofluoroethers: Reactivity toward OH, UV Spectra, and IR Absorption Cross Sections

Vladimir L. Orkin,*,† Eric Villenave,‡ Robert E. Huie, and Michael J. Kurylo

Physical and Chemical Properties Division, National Institute of Standards and Technology, Gaithersburg, Maryland 20899

Received: May 26, 1999; In Final Form: September 28, 1999

The rate constants for the reactions of OH radicals with the fluorinated ethers, $CHF_2-O-CHF_2$ (HFOC-134) and $CF_3CH_2-O-CH_2CF_3$ (HFOC-356mff), were measured using the flash photolysis resonance fluorescence technique over the temperature range 277−370 K to give the following Arrhenius expressions: $k_{\text{HFOC-134}}(T) = (0.63^{+0.20}_{-0.16}) \times 10^{-12} \exp\{-(1646 \pm 76)/T\}$ cm^3 molecule^{-1} s^{-1}, $k_{\text{HFOC-356mff}}(T) = (2.32^{+0.46}_{-0.41}) \times 10^{-12} \exp\{-(790 \pm 47)/T\}$ cm^3 molecule^{-1} s^{-1}. On the basis of the analysis of the available experimental results, the following Arrhenius expression can be recommended for the rate constant of the reaction between OH and HFOC-134: $k_{\text{HFOC-134}}(T) = (0.82^{+0.34}_{-0.24}) \times 10^{-12} \exp\{-(1730 \pm 110)/T\}$ cm^3 molecule^{-1} s^{-1}. Atmospheric lifetimes were estimated to be 24.8 years for HFOC-134 (23.8 years based on the results of this study alone) and 0.3 years for HFOC-356mff. Infrared absorption cross sections of HFOC-134, HFOC-356mff, and HFOC-125 (CHF_2-O-CF_3) were measured at $T = 295$ K from 500 to 1600 cm^{-1} and the global warming potentials of the three compounds were estimated. Ultraviolet absorption spectra of the ethers were measured between 160 and 220 nm. The general pattern of reactivity of hydrofluoroethers toward OH is discussed.

Introduction

Because of the role of chlorofluorocarbons (CFCs) in stratospheric ozone depletion, a large number of replacement compounds, such as hydrochlorofluorocarbons (HCFCs) and hydrofluorocarbons (HFCs), have been selected for industrial applications. The search for CFC alternatives has also focused on oxygen-containing compounds such as partially fluorinated ethers (HFOCs) which, by virtue of not containing any chlorine or bromine, do not contribute to ozone depletion. Nevertheless, the infrared absorbing properties of such fluorinated compounds raise concerns about their role as potential greenhouse gases. The assessment of the global warming potential (GWP) of a compound requires the knowledge of both its atmospheric lifetime and infrared absorption cross sections in the "atmospheric transparency window" between ca. 8 and 12 μm. The atmospheric lifetime of a hydrogen-containing compound is mainly dictated by its reaction with OH radicals in the troposphere. Ultraviolet photolysis can also be important in the case of compounds with low reactivity toward OH however.

In contrast to HCFCs and HFCs, there is very little information on reactivity of partially fluorinated ethers toward hydroxyl radicals.[1−7] Only a few measurements have been reported on the temperature dependence of such rate constants[3−5] to derive Arrhenius parameters as well as rate constants at the temperatures important for atmospheric calculations. We report here the experimental determinations of the rate constants for the reactions of OH with two symmetrical hydrofluoroethers, $CHF_2-O-CHF_2$ (HFOC-134) and $CF_3CH_2-O-CH_2CF_3$ (HFOC-356mff), over the temperature range 277−370 K. Ultraviolet absorption cross sections of HFOC-134, HFOC-356mff, and HFOC-125 (CHF_2-O-CF_3) were measured over the wavelength range 160−220 nm to ascertain the effect of fluorination on the UV spectra of ethers and to estimate the possible role of UV solar absorption on their atmospheric lifetimes. Infrared spectra between 500 and 1600 cm^{-1} were measured for HFOC-134, HFOC-356mff, and HFOC-125 (CHF_2-O-CF_3), and integrated band intensities are reported here as well as the estimated global warming potentials (GWPs) of the three compounds.

Experimental Section

Detailed descriptions of the apparatus and the experimental methods employed in the present work are given elsewhere.[8−10] Thus, only brief overview is given here. Certain commercial equipment, instruments, or materials are identified in this article in order to adequately specify the experimental procedure. Such identification does not imply recognition or endorsement by the National Institute of Standards and Technology, nor does it imply that the material or equipment identified are necessarily the best available for the purpose.

OH Reaction Rate Constant Measurements. The principal component of the flash photolysis/resonance fluorescence (FP/RF) apparatus is a Pyrex reactor (of approximately 50 cm^3 internal volume) thermostated via a fluid circulated through its outer jacket. The reaction was studied in argon carrier gas (99.9995% purity) at a total pressure of 13.33 kPa (100.0 Torr). Dry argon, argon bubbled through water thermostated at 276 K, and HFOC-134 (or HFOC-356mff, 2.00% volume fraction in argon) were premixed and flowed through the reactor at a total flow rate of 0.3 cm^3 s^{-1} to 1.4 cm^3 s^{-1}, STP. The concentrations of the gases in the reactor were determined by measuring the mass flow rates and the total pressure using a MKS Baratron manometer. Flow rates of both argon and the H_2O/Ar mixture were measured using calibrated Tylan mass

† Also associated with the Institute of Energy Problems of Chemical Physics, Russian Academy of Sciences, Moscow, 117829, Russia.

‡ Present address: Laboratoire de Physico-Chimie Moléculaire CNRS UMR 5803, Université Bordeaux I, 351, Cours de la Libération, 33405 Talence Cedex, France.

10.1021/jp991741t CCC: $18.00
Published on Web 11/11/1999

TABLE 1: Summary of the Results Obtained for the Reactions of OH with $CHF_2-O-CHF_2$ (HFOC-134) and $CF_3-CH_2-O-CH_2-CF_3$ (HFOC-356mff)

temperature, K	$[CHF_2OCHF_2]$, 10^{16} molecule/cm^3	$k_{HFOC-134} \times 10^{15}$,[a] cm^3 molecule^{-1} s^{-1}	$[CF_3CH_2OCH_2CF_3]$, 10^{14} molecule/cm^3	$k_{HFOC-356mff} \times 10^{13}$,[a] cm^3 molecule^{-1} s^{-1}
277	1.1−3.9	1.70 ± 0.15 (2)	1.3−4.9	1.35 ± 0.09 (4)
298	0.57−2.6	2.47 ± 0.12 (4)	0.50−3.5	1.63 ± 0.03 (12)
323	0.60−1.8	3.77 ± 0.35 (1)	1.0−3.2	1.93 ± 0.17 (4)
349	0.35−1.06	5.67 ± 0.52 (1)	0.75−2.7	2.38 ± 0.19 (3)
370	0.25−0.85	7.48 ± 0.45 (2)	0.65−2.3	2.77 ± 0.12 (6)

[a] Error bars are levels of confidence of 95% and do not include estimated systematic errors of 4% (see text). Numbers in parentheses indicate the number of experimental measurements.

flow meters, whereas that of the HFOC-134 (or the HFOC-356mff/Ar mixture) was determined by direct measurements of the rate of pressure change in a calibrated volume. The ranges of hydrofluoroethers concentrations are presented in Table 1. The partial pressure of H_2O in the reactor was ca. 0.08 Torr (0.01 kPa) in the experiments presented in Table 1 and up to ca. 2 Torr (0.27 kPa) in some test experiments. Hydroxyl radicals were produced by the pulsed photolysis (0.7−4.2 Hz repetition rate) of H_2O (introduced via the 276 K H_2O/Ar bubbler) using a xenon flash lamp focused into the reactor. The radicals were then monitored by their resonance fluorescence near 308 nm, excited by a microwave-discharge resonance lamp (280 Pa or 2.1 Torr of a ca. 2% volume fraction of H_2O in ultrahigh purity helium) focused into the reactor center. The resonance fluorescence signal was recorded on a computer-based multichannel scanner (channel width 100 μs) as a summation of 1000−22000 consecutive flashes. The radical decay signal at each reactant concentration ([HFOC-134] or [HFOC-356mff]) was analyzed as described by Orkin et al.[9] to obtain the first-order decay rate due to the reaction under study.

UV Absorption Spectra Measurements. The absorption spectra of several ethers and fluoroethers were measured over the wavelength range of 160−220 nm using a single beam apparatus consisting of a 1 m vacuum monochromator equipped with a 600 lines/mm grating. The radiation source was a Hamamatsu L1385 deuterium lamp, and the detector was a Hamamatsu R166 photomultiplier. Spectra were recorded at increments of either 0.5 or 0.1 nm at spectral slit widths of 0.5 and 0.1 nm. The pressure inside the 16.90 ± 0.05 cm absorption cell was measured using full scale 10 and 1000 Torr MKS Baratron manometers at $T = 295 \pm 1$ K. Absorption spectra of the evacuated cell and of the cell filled with a gas sample were alternately recorded several times and the absorption cross sections were calculated from the differences. The complete spectra were constructed from data taken over several overlapping wavelength ranges. Data over each range were obtained at several pressures to verify adherence to the Beer−Lambert absorption law. The spectra were measured at the following compound pressures in the cell: HFOC-134, HFOC-125 (100−900 Torr/13.3−120 kPa); HFOC-356mff (0.5−120 Torr/67 Pa to 16 kPa); dimethyl ether (0.1−900 Torr/13 Pa to 120 kPa); diethyl ether (0.1−400 Torr/13 Pa to 53.3 kPa). The overall instrumental error associated with uncertainties in the path length, pressure, temperature stability, and measured absorbance was estimated to be less than 2% over most of the wavelength range, increasing to approximately 5−10% at the long-wavelength ends of the spectra.

IR Absorption Cross Section Measurements. The spectra were obtained between 500 and 1600 cm^{-1} using a Bruker IFS-66v Fourier transform spectrophotometer. The spectrophotometer, including the cell compartment, was evacuated to less than 10 mPa using a turbomolecular pump in order to minimize errors due to water vapor absorption. All the data presented were measured with ca. 0.12 cm^{-1} spectral resolution. A 20.15 ± 0.05 cm glass absorption cell fitted with KBr windows was used to obtain absorption spectra at the temperature $T = 295 \pm 1$ K. Between spectrum measurements, the cell was pumped out down to ca. 10 mPa using a turbomolecular pump and filled with the gas to be studied two to three times. Sample pressures were measured using full scale 10 and 1000 Torr MKS Baratron manometers. Data over each absorption band range were obtained at several pressures to verify adherence to the Beer−Lambert absorption law. The overall instrumental error associated with uncertainties in the path length, pressure, temperature stability, and the measured absorbance was estimated to be less than 2% over the wavenumber range, increasing below 600 cm^{-1} for weak bands because of residual water vapor absorption.

Absorption spectra of the evacuated cell and the cell filled with the ether under study were recorded sequentially to calculate the absorption cross sections from their differences at different ether concentrations using the Beer−Lambert law,

$$\sigma_{HFOC}(\nu) = \frac{2.303}{[HFOC]L}\{A_{HFOC}(\nu) - A_0(\nu)\} \qquad (1)$$

where $\sigma(\nu)$ is the absorption cross section at wavenumber ν, in units of cm^2 molecule^{-1}; $A_{HFOC}(\nu)$ and $A_0(\nu)$ are absorbancies (base 10) in the presence of ether and that of the evacuated cell at wavenumber ν, as measured with the spectrophotometer; [HFOC] is the concentration of the ether under study, in units of molecule/cm^3; and L is the optical path length in centimeters. A spectrum for each absorption band was recorded at a few different pressures suitable for that band; the maximum absorbance did not exceed $A_{HFOC}(\nu) = 0.7$. The IR measurements were done at the following sample pressures in the cell: HFOC-134 (0.2−8 Torr/27 Pa to 1.1 kPa); HFOC-356mff (0.2−16 Torr/27 Pa to 2.1 kPa); HFOC-125 (0.4−6 Torr/ 53 Pa to 0.8 kPa). Linear least-squares fits were applied to all sample pressure measurements in order to obtain absorption cross sections as well as integrated band intensities. Any measured absorption band with an IBI greater than 0.2% of the highest IBI was attributed to the IR absorption spectra of the compound under study.

All the MKS Baratron manometers used for the OH reaction rate constant measurements (measurements of the pressure in the cell and the ether flow rate), UV absorption measurements, and IR absorption measurements were calibrated and intercompared by measuring the same argon pressure to be identical within less than 0.5% over the whole pressure range.

Sample Purity. The sample of $CHF_2-O-CHF_2$, HFOC-134, was obtained from Hampshire Chemical Co. with a stated purity of 99.97%. Our GC and GC/MS analysis of this sample indicated ca. 99.8% purity with the main impurities, CF_3FCl (ca. 17%), CH_3OH (ca. 0.007%), and CHF_2OCH_2F (ca. 0.027%), with trace amounts of CHF_3 and water. Two samples of $CF_3CH_2-O-CH_2CF_3$, HFOC-356mff, were obtained from

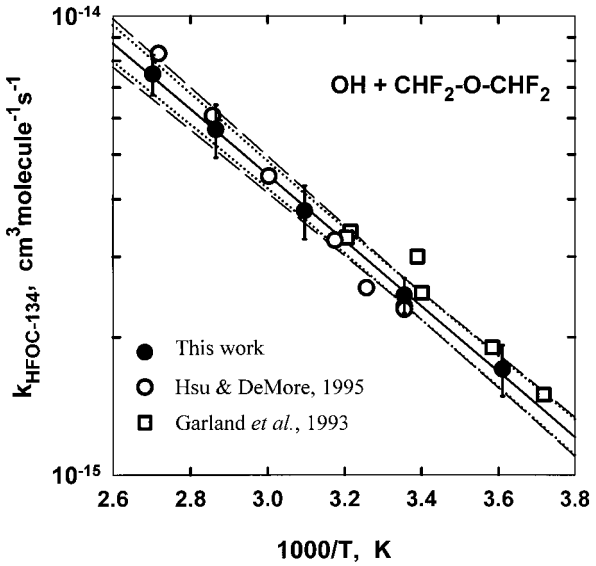

Figure 1. Arrhenius plot showing the average values obtained for $k_{HFOC-134}$ at each temperature. The error bars at each temperature represent the 95% confidence intervals and include the estimated systematic error. The solid line is a least-squares fit to the individual data points that make up these average values. The dotted lines bracket the 95% confidence intervals rigorously obtained from the statistical fit while the dashed lines are from eqs 2 and 2a in the text; both include our estimate of possible systematic errors.

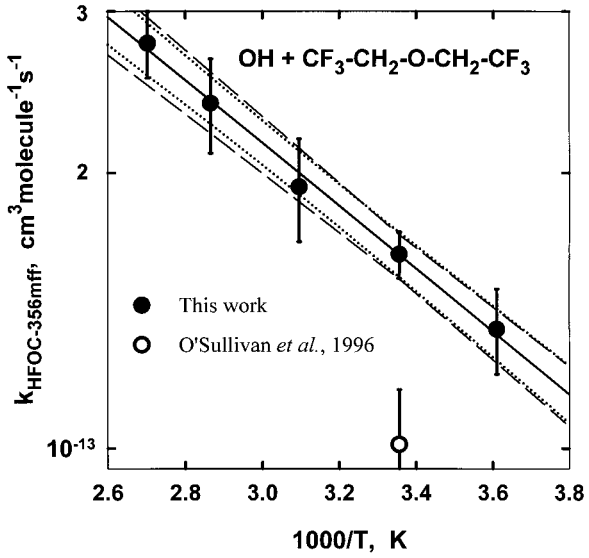

Figure 2. Arrhenius plot showing the average values obtained for $k_{HFOC-356mff}$ at each temperature. The error bars at each temperature represent the 95% confidence intervals and include the estimated systematic error. The solid line is a least-squares fit to the individual data points that make up these average values. The dotted lines bracket the 95% confidence intervals rigorously obtained from the statistical fit while the dashed lines are from eqs 3 and 3a in the text; both include our estimate of possible systematic errors.

Aldrich Chemical Co., each with a stated purity of 99.5+% with CF_3CH_2OH as a main possible impurity. Our analysis of the first sample indicated in ca. 99.87% purity with ca. 0.035% of water, 0.017% of trifluoroethanol, and 0.076% of nonidentified fluorinated impurity, probably a fluoroether. The second sample was ca. 99.7% purity based on our analysis with ca. 0.1% of water and ca. 0.2% of trifluoroethanol as main impurities.

A preparative scale gas chromatograph was used for purification of original samples from the detected impurities. The GC purification of the original samples resulted in no reliably detectable impurities in the purified samples of both HFOC-134 and HFOC-356mff, except residual water, which could also come from a detection system injector. This indicates that the concentrations of all detected impurities were decreased by a factor of at least 20−200.

Results and Discussion

Results of the OH reaction rate constant determinations averaged at each temperature are presented in Table 1 and Figures 1 and 2. Table 2 presents the Arrhenius parameters derived from the fitting to the individual rate constants obtained in our experiments at each temperature as well as the parameters obtained from the fitting of data from other laboratories.

Experiments summarized in Table 1 were performed with GC purified samples of ethers at low flash energy. Test experiments were performed at $T = 298$ K to check possible complications due to any "secondary" chemistry or reactions with impurities. These complications and test experiments are carefully discussed in our previous paper.[10] The initial concentration of OH radicals was changed by either variation of the photolysis flash energy (variation of an electrical energy from 0.3 to 3.3 J) or variation of H_2O concentration in the reactor (a factor of 10). No statistically significant changes in the measured rate constants were obtained. In addition, no dependence of the rate constant on the flash repetition rate by a factor of 4 was discernible. This indicates that "secondary" reactions with radicals formed either in the reactions under study or due to photolysis of reactants do not affect the results of our measurements.

The possible reactions of OH with reactive impurities in the reagent samples can cause the rate constant overestimation especially for reagents having low reactivity toward OH. The error due to the presence of identified impurities can be estimated based on impurity levels and the rate constant of their reactions with OH. In the case of original HFOC-134 sample such estimation indicates that ca. (5−6)% overestimation of the room temperature rate constant would have occurred. The GC purification of the original sample resulted in no reliably detectable impurities in the purified sample of HFOC-134. Thus, the impurity levels in the GC purified sample are low enough to cause no problems in the rate constant measurements. In addition, 21 experiments were done with the original sample before purification which resulted in $k_{HFOC-134}(298) = (2.74 \pm 0.08) \times 10^{-15}$ cm^3 molecule^{-1} s^{-1} vs $k_{HFOC-134}(298) = (2.52 \pm 0.07) \times 10^{-15}$ cm^3 molecule^{-1} s^{-1} in the case of the purified sample. This difference, although only slightly exceeding the overall statistical confidence interval of the measurements, is reasonably consistent with the 5−6% overestimation mentioned above. Hence, the reduction of impurities by more than an order of magnitude should yield results for the purified sample of $CHF_2-O-CHF_2$ that are free from systematic errors due to impurities.

Although we could not identify all detected impurities in the sample of HFOC-356mff, the higher reactivity of this ether makes impurity effects less important. For example, even the highest level (0.2%) of CF_3CH_2OH could result in ca. 0.2% rate constant overestimation based on its reaction rate constant[11] of 1×10^{-13} cm^3 molecule^{-1} s^{-1}. Similarly, the rate constant for the reaction of OH with diethyl ether,[12] 1.3×10^{-11} cm^3 molecule^{-1} s^{-1}, can be used to estimate a conservative upper limit for possible errors due to reaction with a fluoroether impurity. Such errors are not expected to exceed 6% for the original sample and become negligible in the case of GC purified one. Therefore, detected impurities could not be a source of

TABLE 2: Summary of Measurements of $k_{HFOC-134}$ and $k_{HFOC-356mff}$

molecule (HFOC)	temperature range, K	$A \times 10^{12}$, cm^3 molecule^{-1} s^{-1}	$E/R \pm \Delta E/R$, K	$k_{HFOC}(298) \times 10^{14}$, cm^3 molecule^{-1} s^{-1}	reference
$CHF_2-O-CHF_2$ (HFOC-134)	269−312	0.54 ± 0.35[a]	1560 ± 200[a]	0.29 ± 0.02[a]	Garland et al.[3]
		$0.55^{+1.1}_{-0.37}$[b]	1583 ± 322[b]	0.27 ± 0.02[b]	Garland et al.[3,b]
	298−368	$1.9^{+1.2}_{-0.8}$[c]	2007 ± 162[c]	0.23 ± 0.013[c]	Hsu & DeMore[5]
	277−370	$0.63^{+0.20}_{-0.16}$	1646 ± 76	0.252 ± 0.017[d]	this work
$CF_3-CH_2-O-CH_2-CF_3$ (HFOC-356mff)	298			10.1 ± 1.5[e]	O'Sullivan et al.[6]
	277−298	$2.32^{+0.46}_{-0.41}$	790 ± 47	16.3 ± 0.9[d]	this work

[a] All values with their 2σ error bars are taken from the original paper. [b] Results of our fitting to the data set presented in the original paper. Error bars are 95% confidence intervals from the statistical fitting and do not reflect any systematic error. [c] Error bars were derived by fitting of the data set from the original paper and represent 95% confidence intervals. They include neither any possible systematic error nor any uncertainty associated with the rate constant of the reference reaction between OH and CH_3-CCl_3. [d] All error bars indicated include estimated systematic errors of 4%. To obtain the rate constant uncertainties at any temperature, eqs 2a or 3a, given in the text, can be used. [e] The result of a relative rate constant measurement. The reference reaction is not reported. The rate constant and its uncertainty are as quoted by authors.

the error in our experiments with HFOC-356mff. In support of this conclusion, we note that nine experiments using the original sample resulted in $k_{HFOC-356mff}(298) = (1.68 \pm 0.09) \times 10^{-13}$ cm^3 molecule^{-1} s^{-1} (seven measurements) and $k_{HFOC-356mff}(277) = (1.44 \pm 0.20) \times 10^{-13}$ cm^3 molecule^{-1} s^{-1} (two measurements), statistically the same as in the case of GC purified samples (see Table 1).

The expressions for the rate constants and the uncertainty of the rate constants can be written in the manner chosen by the NASA Panel for Data Evaluation, as we have described previously.[9] The Arrhenius parameters were obtained from the linear fitting for log k_i vs $1/T$ data sets (see eqs 2 and 3). Therefore, the uncertainties in thus-determined rate constants should be presented as the uncertainty factors rather than the absolute errors at any temperature. The uncertainty factors can be approximated as given in eqs 2a and 3a:

$$k_{HFOC-134}(T) = 2.52 \times 10^{-15} \exp\left\{-1646\left(\frac{1}{T} - \frac{1}{298}\right)\right\} \text{ cm}^3 \text{ molecule}^{-1} \text{ s}^{-1} \quad (2)$$

$$f(T)_{HFOC-134} = 1.028 \exp\left\{76\left|\frac{1}{T} - \frac{1}{298}\right|\right\} + 0.04 \cong 1.068 \exp\left\{76\left|\frac{1}{T} - \frac{1}{298}\right|\right\} \quad (2a)$$

$$k_{HFOC-134}(T) = 1.62 \times 10^{-13} \exp\left\{-793\left(\frac{1}{T} - \frac{1}{298}\right)\right\} \text{ cm}^3 \text{ molecule}^{-1} \text{ s}^{-1} \quad (3)$$

$$f(T)_{HFOC-356mff} = 1.017 \exp\left\{47\left|\frac{1}{T} - \frac{1}{298}\right|\right\} + 0.04 \cong 1.057 \exp\left\{47\left|\frac{1}{T} - \frac{1}{298}\right|\right\} \quad (3a)$$

Here we have included an estimated systematic uncertainty of 4% as well as the statistical uncertainty factors $f(298)_{HFOC-134} = 1.028$ and $f(298)_{HFOC-356mff} = 1.017$, respectively, at $T = 298$ K obtained from the Arrhenius fitting to the entire data sets. All the uncertainties in both $k_i(298)$ and E/R represent 95% confidence intervals associated with the statistical fitting procedure. The acceptability of the above presentation of the uncertainties (eqs 2a and 3a) is illustrated in Figures 1 and 2 in which we show both the rigorously computed 95% confidence intervals of the regression lines (dotted lines) as well as those approximated using eqs 2a and 3a (dashed lines). Both include the 4% estimated systematic error as a summand. One can see that the uncertainty factors well describe the confidence intervals, especially below room-temperature range, which is important for atmospheric modeling purposes.

The rate constant for the reaction of OH with $CHF_2-O-CHF_2$ was measured previously using a flash photolysis/resonance fluorescence technique by Zhang et al.,[2b] a laser photolysis/laser fluorescence technique by Garland et al.,[3] and a relative technique with OH + CH_3-CCl_3 as a reference reaction by Hsu and DeMore.[5] Table 2 shows the 95% confidence intervals obtained from an Arrhenius fitting of the data presented in the original papers.[3,5] We have not included the room-temperature data from ref 2b in the table since the rate constant obtained, $k(296) = 2.5 \times 10^{-14}$ cm^3 molecule^{-1} s^{-1}, is an order of magnitude higher than those from other measurements and is most likely due to the presence of unresolved reactive impurities in the ether sample. (Our analysis of the data from ref 3 resulted in slightly different Arrhenius parameters and the rate constant at 298 K than those derived by Garland et al. (see Table 2)). Both the A factor and E/R derived by Hsu and DeMore[5] are significantly higher than those derived by Garland et al.[3] The presence of reactive impurities in the sample used by Garland et al. has been suggested by Hsu and DeMore to be a reason for such a discrepancy.

Similar differences exist between the Arrhenius parameters from the present study and those of Hsu and DeMore. However, we paid particular attention to the sample purity. In fact, differences in Arrhenius parameters derived from sets of rate constant data covering only narrow temperature ranges can be misleading. A comparison of the actual rate constants over the common temperature range of study is more appropriate. This is shown in Figure 1 where one can see that our data are in good agreement (better than 15%) with those obtained in ref 5 over entire common temperature range. In particular, our value at $T = 298$ K is not statistically different from that of ref 5, especially when the uncertainty associated with the reference rate constant used in the relative rate study is included. At the high temperature, however, the relative technique data begin to diverge from those of the present study (becoming about 13% higher at $T = 370$ K and leading to the calculation of larger values for both A and E/R than derived from the present results). This difference cannot be explained by the presence of reactive impurities in our study since impurity contamination would cause greater deviations at the lower temperatures. Thus, the differences in the derived Arrhenius parameters are probably due to data scattering (i.e., random errors) or to some systematic errors in one or both of the studies.

The result presented by O'Sullivan et al.[6] appears to be the only available measurement of the rate constant for the reaction between OH and $CF_3-CH_2-O-CH_2-CF_3$. Unfortunately, there is no detailed information on the measurements presented in ref 6 and the reason for the large discrepancy (a factor of 1.6)

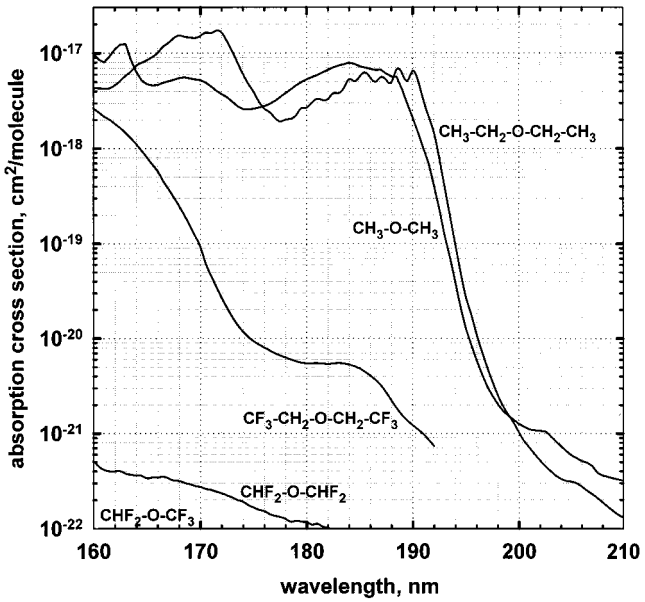

Figure 3. Ultraviolet absorption spectra of several ethers at $T = 295$ K. (The absorption cross sections of CHF_2-O-CF_3 (HFOC-125) were found to be less than 10^{-22} cm^2 molecule^{-1} over the entire spectral range.)

is not clear. As discussed above, we are confident that our measurements are not complicated by either reaction with impurities in the sample or by secondary chemistry.

UV Absorption Spectra. Measured UV absorption spectra of several ethers are presented in Figure 3. For comparison, we have measured the absorption spectra of nonfluorinated analogues as well.

The measurements of the short-wavelength absorption spectra of both CHF_2-O-CF_3 and $CHF_2-O-CHF_2$ were affected by the residual water vapor absorption. We used low-temperature distillation with a cold trap temperature from −80 to −100 °C in order to remove the residual water from the samples. Thus, we can conclude that the absorption cross sections of CHF_2-O-CF_3 are below 10^{-22} cm^2 molecule^{-1} over the entire range of measurements. On the basis of this result, as well as on an identical purification procedure, we are reasonably certain that the absorption spectrum obtained for $CHF_2-O-CHF_2$ is not affected by an impurity. The reproducibility of $CF_3-CH_2-O-CH_2-CF_3$ absorption measurements at wavelengths longer than ca. 190 nm was poor, possibly due to compound adsorption at the optical windows at near saturated vapor pressure. Therefore, we can give only the upper limit of 10^{-21} cm^2 molecule^{-1} for the absorption cross sections over the stratospheric transparency window near 200 nm.

In contrast to alkanes, ethers without fluorine substitution exhibit strong absorption at the wavelengths below 200 nm. This is drastically reduced by fluorination; even fluorination of the carbon atom in the β position with respect to the ether linkage results in a significant decrease of the ether absorptivity. The decrease is more pronounced when the adjacent carbon is fluorinated.

Therefore, fluorinated ethers do not appreciably absorb ultraviolet radiation in the spectral range above 190 nm that can be important for atmospheric implications. The negligible absorbance of fluorinated ethers in the spectral range important for atmospheric implications was also indicated by Orkin et al.[4b]

IR Absorption Cross Sections. The high-resolution infrared spectra of fluorinated ethers obtained in this work did not exhibit any evidence of well-resolved fine rotational structure that could affect the accuracy of the absorption cross section or band intensity measurements. This is not an unexpected result for the compounds containing few heavy halogen atoms in the molecule as will be discussed in a subsequent publication.[13] The integrated band intensities for such molecules can thus be measured without any special spectrum broadening procedure.[13]

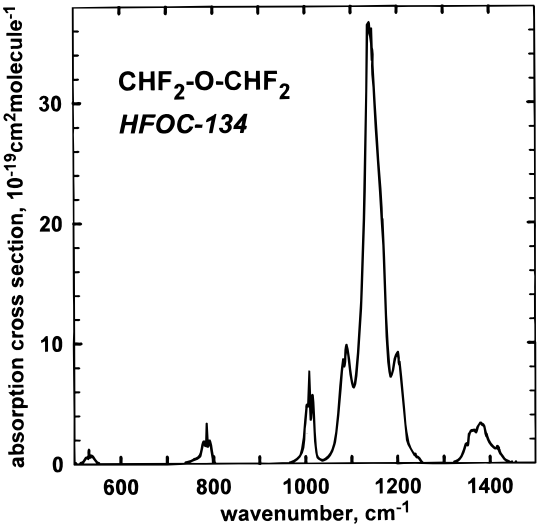

Figure 4. Infrared absorption cross sections of $CHF_2-O-CHF_2$ (HFOC-134) at $T = 295$ K.

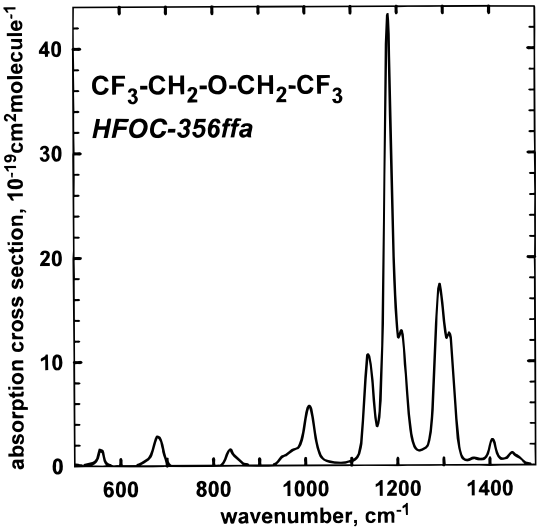

Figure 5. Infrared absorption cross sections of $CF_3-CH_2-O-CH_2-CF_3$ (HFOC-356mff) at $T = 295$ K.

The IR spectra measured for three fluorinated ethers are shown in Figures 4−6. Table 3 lists the integrated band intensities of the main features of the measured IR absorption spectra. The integrated band intensities (IBI) were calculated as follows:

$$\mathrm{IBI}_{\mathrm{HFOC}}(\nu_1 - \nu_2) = \int_{\nu_1}^{\nu_2} \sigma_{\mathrm{HFOC}}(\nu)\, \mathrm{d}\nu \qquad (4)$$

The units of IBI are cm^2 molecule^{-1} cm^{-1}. The indicated band intervals were chosen simply to separate spectral features and compare the IBI with those available from the literature. The absorption cross sections as well as integrated band intensities for the spectral regions were determined from plots of the integrated areas versus hydrofluoroether concentrations. Figure 7 shows examples of such dependencies for the most intense absorption bands.

TABLE 3: Integrated Band Intensities of HFOC-134, HFOC-125, HFOC-356mff

molecule (compound)	integration limits, cm^{-1}	IBI, 10^{-17} cm^2 $molecule^{-1}$ cm^{-1}			
		this work[a]		ref 15	ref 16
$CHF_2-O-CHF_2$ (HFOC-134)	515−552	0.193 ± 0.006			
	600−710	0.047 ± 0.015			
	741−803	0.531 ± 0.008			0.39 ± 0.05
	965−1035	1.315 ± 0.009	{24.90 ± 0.03}		
	1035−1253	21.728 ± 0.030			25.18 ± 0.41
	1322−1443	1.855 ± 0.011			
$CF_3-CH_2-O-CH_2-CF_3$ (HFOC-356mff)	500−600	0.307 ± 0.007			
	600−740	0.798 ± 0.019			
	780−900	0.389 ± 0.013			
	900−1070	2.328 ± 0.017			
	1070−1250	15.605 ± 0.062			
	1250−1350	7.130 ± 0.035			
	1350−1600	1.162 ± 0.032			
CHF_2-O-CF_3 (HFOC-125)	555−670	0.229 ± 0.009			0.58 ± 0.02
	700−785	0.225 ± 0.015		0.209 ± 0.01	
	785−830	(0.025 ± 0.007)[b]			0.03 ± 0.01
	830−860	(0.009 ± 0.001)[b]			
	860−980	0.962 ± 0.020		0.949 ± 0.01	0.93 ± 0.04
	980−1143	5.746 ± 0.027	{31.22 ± 0.07}	32.3 ± 0.40	31.3 ± 1.09
	1143−1184	4.465 ± 0.010			
	1184−1266	13.123 ± 0.053			
	1266−1343	6.804 ± 0.022			
	1343−1450	0.999 ± 0.022			
	1450−1510	0.080 ± 0.008			

[a] IBI values and their 95% confidence intervals shown in the table were obtained from the linear fitting of the integrated absorption areas versus hydrofluoroether pressure and do not include the estimated systematic error of ca. 2%. [b] The weak absorption band was not originally included in Table 3 to be assigned to the IR spectrum of CHF_2-O-CF_3. The value is shown to compare with that by Heathfield et al.[16]

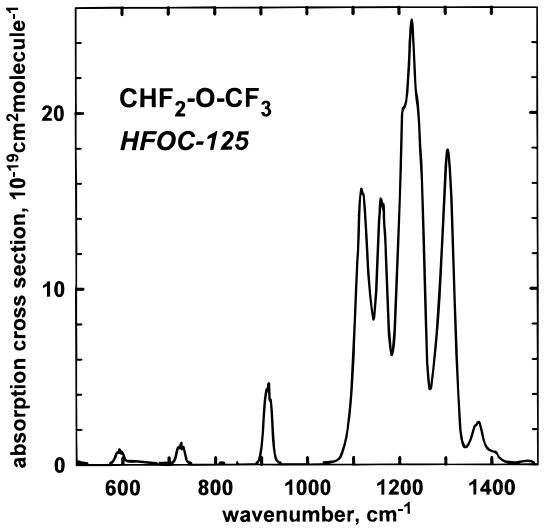

Figure 6. Infrared absorption cross sections of CHF_2-O-CF_3 (HFOC-125) at $T = 295$ K.

There are three papers reporting integrated band intensities measured for these three hydrofluoroethers.[14−16] Only the total integrated absorption intensity of HFOC-125 over the entire range between 450 and 2000 cm^{-1} measured with a spectral resolution of 0.5 cm^{-1} is presented in ref 14. The reported value of 29.22 cm^2 $molecule^{-1}$ cm^{-1} is significantly smaller than our total value of 32.64 cm^2 $molecule^{-1}$ cm^{-1} for the same range. Results from two other studies[15,16] reporting the integrated band intensities for different absorbing bands of HFOC-125 and HFOC-134 are listed in Table 3 for comparison with our data. These two studies of CHF_2-O-CF_3 were performed using different spectral resolutions. Heathfield et al.[15] employed resolutions of 0.03 and 0.1 cm^{-1} to measure the absorption of nondiluted ether samples. Heathfield et al.[16] used the higher resolution of 0.0032 cm^{-1} to study the nitrogen-diluted samples.

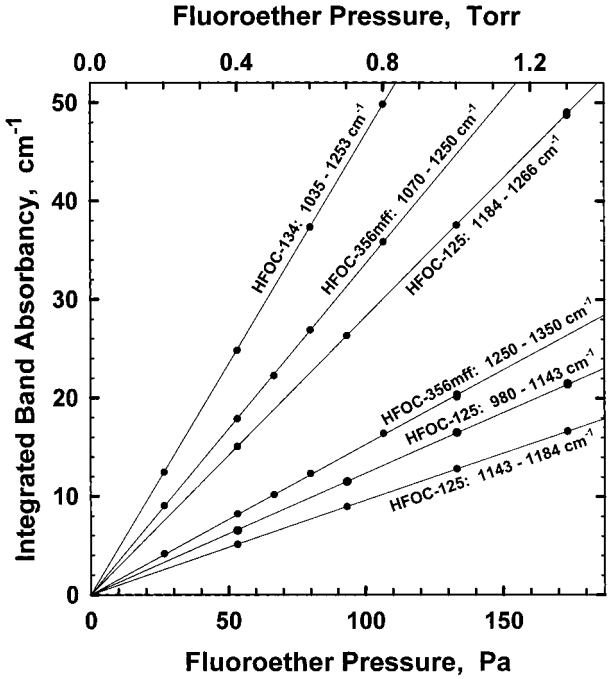

Figure 7. Dependence of the integrated absorption in several of the strongest bands (base 10) on the hydrofluoroether pressure.

One can see the excellent agreement between all measurements for the main absorption bands, while some discrepancies exist for the weakest ones. The agreement confirms our conclusion that neither pressure broadening nor very high resolution are necessary for measuring the midinfrared range absorption spectra of deeply halogenated hydrocarbons.[13] Note that two bracketed absorption band intensities shown in Table 3 did not meet our 0.2% criteria to be assigned to the absorption spectrum of CHF_2-O-CF_3 (since they were only 0.19% and 0.07% of the strongest 1184−1266 cm^{-1} band, respectively). They are

TABLE 4: Relative Radiative Forcing (RRF_{HFOC}^{CFC-11}), Atmospheric Lifetime, HGWP, and GWP for Hydrofluoroethers

compound (molecule)	RRF_{HFOC}^{CFC-11}	atmospheric lifetime, yrs	Global warming potentials at time horizons of: 20 years HGWP	20 years GWP	100 years HGWP	100 years GWP	500 years HGWP	500 years GWP
CFC-11 ($CFCl_3$)	1.00	45[a]	1.0	6300	1.0	4600	1.0	1600
HFOC-134 (CHF_2-O-CHF_2)	1.77[c]	24.8	1.75	11000	1.25	5800	1.14	1820
HFOC-356mff (CF_3-CH_2-O-CH_2-CF_3)	1.54[c]	0.294	0.021	134	0.0086	39	0.0076	12
HFOC-125 (CHF_2-O-CF_3)	1.80[c]	165[b]	2.1	13400	3.4	15600	6.4	10200

[a] The calculated atmospheric lifetime of CFC-11 ($CFCl_3$) and its GWP relative to CO_2 were taken from ref 22. [b] The atmospheric lifetime of CHF_2-O-CF_3 was calculated using eq 5 and the rate constant for the reaction with OH from ref 19. [c] Heathfield et al.[16] reported $RRF_{134}^{CFC-11} = 1.48$ and $RRF_{125}^{CFC-11} = 1.40$; Christidis et al.[14] reported $RRF_{125}^{CFC-11} = 1.55$; Wallington et al.[17] reported $RRF_{356mff}^{CFC-11} = 1.35$. All data are based on results of radiative transfer modeling for the cloudy sky.

included into the table only to compare with the results presented by Heathfield et al.[16] In any case, such disagreement in the weak long-wavelength band intensities does not affect the estimations of the global warming potentials of the compounds.

Garland et al.[3] measured the IR absorption spectrum of HFOC-134 diluted with dry air up to 1 atm total pressure between 770 and 1430 cm^{-1} (the spectral resolution is not reported). Their absorption intensity integrated over the range can be recalculated[16] to give 25.3×10^{-17} cm^2 $molecule^{-1}$ cm^{-1} that coincides with our value of 25.4×10^{-17} cm^2 $molecule^{-1}$ cm^{-1} obtained by integrating over the same wavenumber interval.

The only available IR spectrum of $CF_3-CH_2-O-CH_2-CF_3$ is presented in a figure by Wallington et al.[17] Their absorption cross sections appear to agree with our results as best as can be estimated from an analysis of the published figure. The agreement is probably better than 3% at the main absorption peak at 1181.3 cm^{-1}.

Atmospheric Implications

Reactions with hydroxyl radicals in the troposphere are the main removal processes for hydrogen-containing compounds. Following Prather and Spivakovsky,[18] we can estimate the atmospheric lifetime of an HFOC (τ_{HFOC}) due to reactions with hydroxyl radicals in the troposphere as

$$\tau_{HFOC}^{OH} = \frac{k_{MC}(277)}{k_{HFOC}(277)}\tau_{MC}^{OH} \quad (5)$$

where τ_{HFOC}^{OH} and $\tau_{MC}^{OH} = 5.9$ years are the atmospheric lifetimes of HFOC under study and methyl chloroform (MC), respectively, due to reactions with hydroxyl radicals in the troposphere only, and $k_{HFOC}(277)$ and $k_{MC}(277) = 6.69 \times 10^{-15}$ cm^3 $molecule^{-1}$ s^{-1} (ref 19) are the rate constants for the reactions of OH with these substances at $T = 277$ K. The value of τ_{MC}^{OH} was obtained following the procedure used by Prinn et al.[20] from the measured lifetime of MC, $\tau_{MC} = 4.8$ years when an ocean loss of 85 years and a stratospheric loss of 37 years are taken into account.

Given our earlier discussion of the differences in the Arrhenius parameters for the reaction between OH and $CHF_2-O-CHF_2$ obtained in the present work and reported in ref 5, a fit to the combined data is best recommended. Such a combined fit results in

$$k_{HFOC\text{-}134}(T) = (0.82^{+0.34}_{-0.24}) \times 10^{-12} \exp\{-(1730 \pm 110)/T\} \text{ cm}^3 \text{ molecule}^{-1} \text{ s}^{-1} \quad (6a)$$

$$k_{HFOC\text{-}134}(T) = 2.46 \times 10^{-15} \exp\left\{-1730\left(\frac{1}{T} - \frac{1}{298}\right)\right\} \text{ cm}^3 \text{ molecule}^{-1} \text{ s}^{-1} \quad (6b)$$

$$f(T)_{HFOC\text{-}134} \cong 1.1 \exp\left\{110\left|\frac{1}{T} - \frac{1}{298}\right|\right\} \quad (6c)$$

We did not include the data from ref 3 in this combined fit because of their higher scatter and smaller region of temperature overlap with the other studies. The fit to a data set combined from the results obtained over different temperature ranges can cause additional systematic errors in the Arrhenius parameters.[29] The recommended fit to our data and those of ref 5 results in a rate constant $k_{HFOC\text{-}134}(277) = 1.59 \times 10^{-15}$ cm^3 $molecule^{-1}$ s^{-1} that is ca. 14% higher than the current JPL Data Panel recommendation.[19] For the rate constant of the reaction between OH and $CF_3-CH_2-O-CH_2-CF_3$, we can only recommend expression 3 (which does not include the room-temperature data of ref 6 because of the lack of detailed information on these measurements). The atmospheric lifetimes were thus calculated to be 24.8 years and 0.294 years for HFOC-134 and HFOC-356mff, respectively, based on these recommendations for the rate constants.

All the fluorinated ethers studied here absorb UV radiation in neither the troposphere nor the stratosphere. Therefore, the values of τ_{HFOC}^{OH} are the good estimations of their total atmospheric lifetimes.[9] The calculated atmospheric lifetimes are presented in Table 4 along with our estimations of the radiative forcing and global warming potentials of the compounds.

The measured infrared absorption cross sections together with the estimated atmospheric lifetimes allowed us to estimate the climate related properties of the fluorinated ethers. The calculation technique we used here will be described in detail by Orkin et al.[13] Therefore, we present here only the main equations that were used for the calculations. The experimentally obtained spectrum of the Earth's outgoing infrared radiation[21] was used to calculate the relative radiating forcing of the ether with CFC-11 ($CFCl_3$) as the reference,

$$RRF_{HFOC}^{CFC\text{-}11} = \frac{\int_{\nu_1}^{\nu_2} \sigma_{HFOC}(\nu)\Phi(\nu)\, d\nu}{\int_{\nu_1}^{\nu_2} \sigma_{CFC-11}(\nu)\Phi(\nu)\, d\nu} \quad (6)$$

where $\Phi(\nu)$ is the intensity of outgoing Earth's radiation. We

TABLE 5: Rate Constants for Reactions between Fluorinated Ethers and Corresponding Alkanes

molecule	$A \times 10^{12}$, $cm^3\,molec^{-1}\,s^{-1}$	E/R, K	$k(298) \times 10^{14}$, $cm^3\,molec^{-1}\,s^{-1}$	reference
CH_3-CH_3	7.9	1030	25.0	27
CH_3-O-CH_3	11.0	370	290.0	27
$CH_3-CH_2-CF_3$			4.2	19
$CH_3-O-CH_2-CF_3$			63.0	2, 6
$CH_3-CH_2-O-C_4F_9$			7.0	28
CH_3-CF_3	1.2	2030	0.13	9
$CH_3-C_2F_5$	0.44	1690	0.15	29
CH_3-O-CF_3	1.5	1450	1.2	19
$CH_3-O-C_4F_9$			1.4	30
CH_3-CHF_2	2.4	1260	3.5	19
$CH_3-O-CHF_2$	6.0	1530	3.5	4
CHF_2-CHF_2	1.6	1680	0.57	19
$CHF_2-O-CHF_2$	0.63	1650	0.25	this work
	1.9	2000	0.23	5
CHF_2-CF_3	0.56	1700	0.19	19
CHF_2-O-CF_3	0.47	2100	0.041	19
$CH_3-CH_2-CH_2-CH_3$	9.0	395	240.0	27
$CH_3-CH_2-O-CH_2-CH_3$	5.8	−240	1300.0	12
$CF_3-CH_2-CH_2-CF_3$	3.0	1800	0.71	19
$CF_3-CH_2-O-CH_2-CF_3$	2.3	790	16.2	this work
$CHF_2-CH_2-CF_3$	0.61	1330	0.70	19
$CHF_2-O-CH_2-CF_3$	2.6	1610	1.2	19

used absorption cross sections of $CFCl_3$, $\sigma_{CFC-11}(\nu)$ obtained by Orkin et al.[13] for the calculations.

Time-dependent halocarbon global warming potentials, HGWP(t) (the global warming potential with CFC-11 as a reference compound), were then calculated[13] using the compound atmospheric lifetimes presented in Table 4,

$$\mathrm{HGWP}_{\mathrm{HFOC}}(t) = \frac{M_{\mathrm{CFC-11}}}{M_{\mathrm{HFOC}}} \frac{\int_{\nu_1}^{\nu_2} \sigma_{\mathrm{HFOC}}(\nu)\Phi(\nu)\,\mathrm{d}\nu}{\int_{\nu_1}^{\nu_2} \sigma_{\mathrm{CFC-11}}(\nu)\Phi(\nu)\,\mathrm{d}\nu} \frac{\tau_{\mathrm{HFOC}}}{\tau_{\mathrm{CFC-11}}} \frac{1-\exp(-t/\tau_{\mathrm{HFOC}})}{1-\exp(-t/\tau_{\mathrm{CFC-11}})} = \mathrm{RRF}_{\mathrm{HFOC}}^{\mathrm{CFC-11}} \frac{M_{\mathrm{CFC-11}}}{M_{\mathrm{HFOC}}} \frac{\tau_{\mathrm{HFOC}}}{\tau_{\mathrm{CFC-11}}} \frac{1-\exp(-t/\tau_{\mathrm{HFOC}})}{1-\exp(-t/\tau_{\mathrm{CFC-11}})} \quad (7)$$

where M_{HFOC} and $M_{\mathrm{CFC-11}}$ are molecular weights of the fluoroether and $CFCl_3$, respectively. The hydrofluoroethers studied in the present work have no intense absorption bands that overlap the 15 μm absorption band of carbon dioxide (ca. 600−800 cm^{-1}). Therefore, such calculations should result in reasonable and accurate estimations of the radiative forcing and HGWPs of the compounds.[13]

All the atmospheric parameters discussed above τ_{HFOC}, $\mathrm{RRF}_{\mathrm{HFOC}}^{\mathrm{CFC-11}}$, and $\mathrm{HGWP}_{\mathrm{HFOC}}(t)$ are the results of self-consistent estimations made by using only data from laboratory measurements (k_i, $\sigma_i(\nu)$) and field measurements (τ_{MC}, $\Phi(\nu)$). Global warming potentials with CO_2 as a reference (GWP) cannot be accurately calculated in the above-described manner due to the high concentration of carbon dioxide in the real Earth's atmosphere that results in nonlinear absorption of the outgoing radiation by CO_2 molecules.[13] Therefore, we used the global warming potential of CFC-11 referenced to CO_2 ($\mathrm{GWP}_{\mathrm{CFC-11}}$) calculated using a radiative transfer model of the atmosphere[22] to obtain the GWPs of the ethers presented in Table 4,

$$\mathrm{GWP}_{\mathrm{HFOC}}(t) = \mathrm{HGWP}_{\mathrm{HFOC}}(t)\mathrm{GWP}_{\mathrm{CFC-11}}(t) \quad (8)$$

The latest accepted data for GWPs are presented in the *Scientific Assessment of Ozone Depletion: 1998*.[22] Our estimations for the GWPs of HFOC-125 presented in Table 4 agree with the recommendations from this assessment to better than 3%. Our estimations for the GWPs of HFOC-134 differ from those in ref 22 by between 7% and 21% depending on the time horizon. This difference is entirely due to the difference between the lifetime for HFOC-134 derived here and that used in ref 22. For example, if a lifetime of HFOC-134 of 29.7 years (i.e., the value in ref 22) were used in our calculations, the GWPs derived would agree with those from ref 22 within 2%.

Reactivity of Hydrofluoroethers

Generally, it has been assumed that ethers are more reactive toward hydrogen abstraction than the parent alkanes due to a decrease in the C−H bond strengths, particularly on the carbon adjacent to the ether linkage. Indeed, evidence has been presented indicating the effect of the ether linkage on increasing the reactivity of C−H bonds[2a] as far as four carbons removed from the ether function. Increases in reactivity of a corresponding magnitude have not been observed when a second ether function is present.[23] In fact, the presence of a second ether function in a cyclic ether actually decreases the reactivity of the compound (for example, *p*-dioxane vs tetrahydrofuran).[24] However, early calculations support the idea that this reactivity pattern correctly reflected the differences in the bond strengths.[25] Examination of the current data set for hydrofluoroethers suggests that the inclusion of an ether linkage in a fluoroalkane either does not decrease the C−H bond strength as it does for simple hydrocarbons or that other factors (in addition to C−H bond strength) may be important in determining reactivity patterns.

In Table 5, we present the kinetic parameters for the reactions of OH with hydrofluoroethers and for their parent alkanes. The same results are presented graphically in Figure 8, where the room-temperature rate constants for the alkanes are given on a logarithmic scale on the left and the ethers on the right. The lines drawn connect the corresponding pairs. It is quite evident that the simple assumption of uniform activation of neighboring

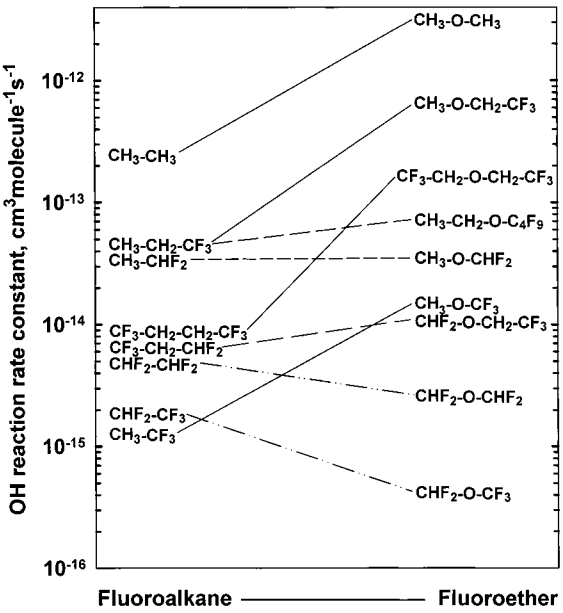

Figure 8. Graph of OH reactivity toward fluoroalkanes and corresponding fluoroethers at $T = 298$ K.

C−H bonds by the ether linkage is not correct. Rather, both activation and deactivation are observed. The net result is that the reactivities of the ethers span a much wider range than the reactivities of the parent alkanes, i.e., an increased spread of about 1.5 orders of magnitude.

It is difficult to discern clear trends from these data. We note that the two hydrofluoroethers, with no fluorine α to the ether linkage, both react significantly faster than their parent alkanes. For ethers where only one of the α carbons is fluorinated, the reactivity ranges from remaining unchanged to increasing by an order of magnitude. On the other hand, decreases in reactivity are observed for the two ethers in which both α carbon atoms are fluorinated. In the absence of a more comprehensive database for hydrofluoroether reactivity, it is difficult to draw conclusions regarding changes in Arrhenius parameters due to the addition of an ether linkage. We are presently performing ab initio calculations of the OH + hydrofluoroether reaction system in an attempt to obtain insight into the energetics and mechanisms for such reactions, with the objective of developing a predictive capability for reactivity toward OH.

Rate constants for the reactions between OH and few other hydrofluoroethers not listed in the Table 5 are also available from the literature. O'Sullivan et al.[6] reported a rate constant of 2.1×10^{-14} cm^3 molecule^{-1} s^{-1} for the reaction between OH and $CH_3-O-CF_2CHFCF_3$. This result is reasonably consistent with the structurally closest reactions in Table 5. Heathfield et al.[7] reported rate constants of 20, 16.5, 9.4, and 43 ($\times 10^{-14}$ cm^3 molecule^{-1} s^{-1}) for the reactions of OH with $CH_3-O-CF_2CHF_2$, CH_3-O-CF_2CHFCl, $CF_3CH_2-O-CF_2CHF_2$, and $CH_3CH_2-O-CF_2CHF_2$, respectively, from a pulse radiolysis experiment. On the basis of the reactivity information presented in Table 5, we conclude that all of them (especially first three reactions) are highly overestimated. Indeed, we expect the reactivity of $CH_3-O-CF_2CHF_2$ to be between that of CH_3-O-CF_3 and $CH_3-O-CHF_2$, i.e., around 2×10^{-14} cm^3 molecule^{-1} s^{-1} (see Table 5). On the basis of the reactivity of closely related haloethanes,[19,26] we conclude that the reactivity of CH_3-O-CF_2CHFCl should be higher than that of $CH_3-O-CF_2CHF_2$, not vice versa. The reactivity of $CF_3CH_2-O-CF_2CHF_2$ is probably close to that of $CF_3CH_2-O-CHF_2$ (see Table 5). The estimation of the reactivity of $CH_3CH_2-O-CF_2-CHF_2$ is not as straightforward. It should slightly exceed the reactivity of $CH_3CH_2-O-C_4F_9$, whereas a factor of 6 (as suggested by the results of Heathfield et al.) seems too high. The presence of reactive impurities in the samples or the reactions with the ether decomposition products in the studies by these authors could be the possible reasons for such overestimation.

Acknowledgment. This work was supported by the Upper Atmosphere Research Program of the National Aeronautics and Space Administration and by the Next Generation Fire Suppression Technology Program, funded by the Department of Defense Strategic Environmental Research and Development Program under MIPR number W74RDV73243630. We thank Dr. Pamela Chu (NIST) for her help in measuring the IR spectra of the compounds.

References and Notes

(1) (a) Brown, A. C.; Canosa-Mas, C. E.; Parr, A. D.; Pierce, J. M. T.; Wayne, R. P. *Nature* **1989**, *341*, 635−637. (b) Brown, A. C.; Canosa-Mas, C. E.; Parr, A. D.; Wayne, R. P. *Atmos. Environ.* **1990**, *24A*, 2499−2511.

(2) (a) Wallington, T. J.; Liu, R.; Dagaut, P.; Kurylo, M. J. *Int. J. Chem. Kinet.* **1988**, *20*, 41−49. (b) Zhang, Z.; Saini, R. D.; Kurylo, M. J.; Huie, R. E. *J. Phys. Chem.* **1992**, *96*, 9301−9304.

(3) Garland, N. L.; Medhurst, L. J.; Nelson, H. H. *J. Geophys. Res.* **1993**, *98*, 23107−23111.

(4) (a) Orkin, V. L.; Khamaganov, V. G.; Guschin, A. G.; Huie, R. E.; Kurylo, M. J. *The 13th International Symposium on Gas Kinetics*; The University College of Dublin, Dublin, Ireland, September 1994; p D56. (b) Orkin, V. L.; Khamaganov, V. G.; Guschin, A. G.; Kasimovskaya, E. E.; Larin, I. K. *Development of Atmospheric Characteristics of Chlorine-Free Alternative Fluorocarbons, Report on R-134a and E-143a*; Report ORNL/Sub/86X-SL103V prepared for the Oak Ridge National Laboratory, 1993. (c) Orkin, V. L.; Khamaganov V. G.; Guschin A. G.; Larin I. K. Manuscript in preparation.

(5) Hsu, K.-J.; DeMore, W. B. *J. Phys. Chem.* **1995**, *99*, 11141−11146.

(6) O'Sullivan, N.; Wenger, J.; Sidebottom, H. In *Proceedings of the 7th European Commission Symposium on Physiochemical Behavior of Atmospheric Pollutants*; Venice, Italy, October, 1996; Larsen, B., Versino, B., Eds.; Office for Official Publications of the European Communities: *Luxenbourg, 1997*; p 77−79.

(7) Heathfield, A. E.; Anastasi, C.; Pagsberg, P.; McCulloch, A. *Atmos. Environ.* **1998**, *32*, 711−717.

(8) Kurylo, M. J.; Cornett, K. D.; Murphy, J. L. *J. Geophys. Res.* **1982**, *87*, 3081−3085.

(9) Orkin, V. L.; Huie, R. E.; Kurylo, M. J. *J. Phys. Chem.* **1996**, *100*, 8907−8912.

(10) Orkin, V. L.; Khamaganov, V. G.; Guschin, A. G.; Huie, R. E.; Kurylo, M. J. *J. Phys. Chem.* **1997**, *101*, 174−178.

(11) Wallington, T. J.; Dagaut, P.; Kurylo, M. J. *J. Phys. Chem.* **1988**, *92*, 5024.

(12) Mellouki, A.; Teton, S.; Le Bras, G. *Int. J. Chem. Kinet.* **1995**, *27*, 791−805.

(13) Orkin, V. L.; Guschin, A. G.; Larin, I. K.; Huie, R. E.; Kurylo, M. J. Manuscript in preparation.

(14) Christidis, N.; Hurley, M. D.; Pinnock, S.; Shine, K. P.; Wallington, T. J. *J. Geophys. Res.* **1997**, *102* (D16), 19597−19609.

(15) Heathfield, A. E.; Anastasi, C.; Ballard, J.; Newnham, D. A.; McCulloch, A. *J. Quant. Spectrosc. Radiat. Transfer* **1998**, *59*, 91−97.

(16) Heathfield, A. E.; Anastasi, C.; McCulloch, A.; Nicolaisen, F. M. *Atmos. Environ.* **1998**, *32*, 2825−2833.

(17) Wallington, T. J.; Guschin, A.; Stein, T. N.; Platz, J.; Sehested, J.; Christensen, L. K.; Nielsen, O. J. *J. Phys. Chem. A* **1998**, *102*, 1152−1161.

(18) Prather, M.; Spivakovsky, C. M. *J. Geophys. Res.* **1990**, *95*, 18723−18729.

(19) DeMore, W. B.; Sander, S. P.; Golden, D. M.; Hampson, R. F.; Kurylo, M. J.; Howard, C. J.; Ravishankara, A. R.; Kolb, C. E.; Molina, M. J. *JPL Publication 97-4*; Jet Propulsion Laboratory, California Institute of Technology: Pasadena, CA, 1997.

(20) Prinn, R. G.; Weiss, R. F.; Miller, B. R.; Huang, A.; Alyea, F. N.; Cunnold, D. M.; Fraser, P. J.; Hartley, D. E.; Simmonds, P. G. *Science* **1995**, *269*, 187−192.

(21) Kunde, V. G.; Conrath, B. J.; Hanel, R. A.; Maguire, W. C.; Prabhakara, C.; Salomonson, V. V. *J. Geophys. Res.* **1974**, *79*, 777−784.

(22) *Scientific Assessment of Ozone Depletion: 1998*; Global Ozone Research and Monitoring Project, Report No. 44; World Meteorological Organization: Geneva, Switzerland, 1999.

(23) Dagaut, P.; Liu, R.; Wallington, T. J.; Kurylo, M. J. *Int. J. Chem. Kinet.* **1989**, *21*, 1173−1180.

(24) Dagaut, P.; Liu, R.; Wallington, T. J.; Kurylo, M. J. *J. Phys. Chem.* **1990**, *94*, 1881−1883.

(25) Huie, R. E.; Clifton, C. L.; Kafafi, S. A. *J. Phys. Chem.* **1991**, *95*, 9336−9340.

(26) Guschin, A. G.; Kasimovskaya, E. E.; Khamaganov, V. G.; Orkin, V. L. *Proceedings of the Workshop on the Atmospheric Degradation of HCFCs and HFCs*; Boulder CO, November 17−19, 1993; p 1−51.

(27) Atkinson, R.; Baulch, D. L.; Cox, R. A.; Hampson, R. F., Jr.; Kerr, J. A.; Rossi, M. J.; Troe, J. *J. Phys. Chem. Ref. Data* **1999**, *28*, 191−393.

(28) Christensen, L. K.; Sehested, J.; Nielsen, O. J.; Bilde, M.; Wallington, T. J.; Guschin, A.; Molina, L. T.; Molina, M. J. *J. Phys Chem. A* **1998**, *102*, 4839−4845.

(29) Orkin, V. L.; Huie, R. E.; Kurylo, M. J. *J. Phys. Chem.* **1997**, *101*, 9118−9124.

(30) Wallington, T. J.; Schneider, W. F.; Sehested, J.; Bilde, M.; Platz, J.; Nielsen, O. J.; Christensen, L. K.; Molina, M. J.; Molina, L. T. *J. Chem. Phys. A* **1997**, *101*, 8264−8274.